Langmuir

Article

pubs.acs.org/Langmuir

Enantiospecific Desorption of *R*- and *S*-Propylene Oxide from D- or L-Lysine Modified Cu(100) Surfaces

Wai Yeng Cheong and Andrew J. Gellman*

Department of Chemical Engineering, Carnegie Mellon University, Pittsburgh, Pennsylvania 15213, United States

Supporting Information

ABSTRACT: The enantiospecific desorption kinetics of *R*- and *S*-propylene oxide (PO) from a Cu(100) surface modified by enantiomerically pure D- or L-lysine have been studied using temperature programmed desorption. These experiments have used *R*- or *S*-PO as the chiral probe for study of enantiospecific adsorption on Cu(100) surfaces modified with D- or L-lysine. This chiral probe/modifier/Cu system manifests a significant diastereomeric effect in the *R*- and *S*-PO peak desorption temperatures and, hence, true enantiospecific behavior. The enantiospecificity in the PO desorption kinetics is observed only over a narrow range of lysine modifier coverage with a maximum at a lysine coverage leaving an empty site density of $\theta_O \approx 0.25$. The observation of enantiospecific behavior in the PO/lysine/Cu(100) system is in contrast with the failed results of prior attempts to observe enantiospecific desorption from chirally modified Cu surfaces. The potential for hydrogen-bonding interactions between the chiral probe and chiral modifier, which can depend on the coverage and configuration of the adsorbed modifier, may play a crucial role in enantiospecific adsorption on lysine modified Cu surfaces.

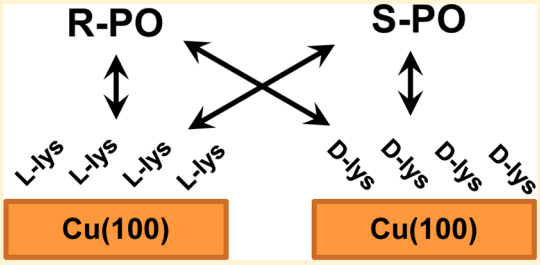

1. INTRODUCTION

The production of enantiomerically pure chiral compounds for use in the pharmaceuticals industry or for other bioactive purposes involves complex and expensive enantiospecific chemical processes. Any chemical reaction that produces a chiral compound from achiral reactants in an achiral environment will yield a racemic mixture of the two product enantiomers. In these cases, the desired enantiomer must then be separated from the undesired enantiomer. Because conventional separation processes exploit differences in bulk physical properties, for example, solubility, boiling point, melting point, density, vapor pressure, and so forth, to separate mixtures, it is impossible to separate enantiomers using these classical separation techniques in an achiral environment. These properties will be identical for both enantiomers in achiral environments. In order to induce enantioselective separation, a chiral medium such as a chiral surface or a chiral solvent must be employed to differentiate the properties of the two enantiomers.

Chiral surfaces can be prepared by a number of methods. Naturally chiral surfaces can be prepared by cleaving crystals along low symmetry directions with no mirror planes normal to the exposed surface. In metals, which have high symmetry achiral bulk structures, the low symmetry, high Miller index planes have structures formed of low Miller index terraces separated by kinked step edges and are chiral.[1−2] The three low Miller index microfacets that form the kinks can be arranged with a clockwise or counterclockwise sense of rotation that determines the chirality (*R*- or *S*-) of the surface. Another approach to fabricating chiral surfaces is through modification of achiral surfaces by adsorption of chiral molecules. These chiral modifiers can impart chirality to the achiral surface by a number of means. First, the adsorbed modifiers can self-assemble into an ordered layer to form a "templated chiral surface". For example, adsorption of *R*,*R*-tartaric acid or L-alanine on the Cu(110) surface results in well-ordered overlayers with structures that break the symmetry of the substrate and impart long-range chirality.[4] It has been hypothesized that these supramolecular adlayer structures contain nanosized chiral pockets which expose the Cu substrate and can serve as chiral sites for enantiospecific adsorption and reaction. Reactant molecules could adsorb with an asymmetric orientation, forcing subsequent reactions to occur enantioselectively. Even without the long-range chirality imparted by the formation of an ordered modifier overlayer, local chirality can be conferred to a surface by the intrinsic chirality of an isolated, adsorbed chiral modifier and the asymmetry of adsorption sites in its immediate vicinity. In this case, enantioselectivity arises from the chiral-directing interaction between the isolated adsorbed modifier and an adsorbed reactant molecule. This type of one-to-one interaction between methyl pyruvate (reactant) and cinchonidine (modifier) is one of the proposed mechanisms for chiral induction in the enantioselective hydrogenation of methyl pyruvate over cinchonidine modified Pt catalysts.[5] The adsorption of chiral organic species can also imprint chirality onto an achiral surface by inducing

Received: July 9, 2012
Revised: September 27, 2012
Published: September 28, 2012

reconstruction of the achiral surface into a naturally chiral structure such as a high Miller index plane which exposes kinked step edges.[6] Such chiral imprinting of achiral surfaces has been observed during adsorption of L-lysine, $HO_2CCH(NH_2)(CH_2)_4NH_2$, on Cu(100).[2,7−9] Under certain conditions, L-lysine adsorbed on Cu(100) can induce the formation of homochiral $(3,1,17)^R$ facets through step bunching and faceting. Although there are many examples of the formation of chiral structures on surfaces by adsorption of various modifiers,[4−15] the observation of enantiospecific adsorption of chiral probes onto these chiral surfaces is much more challenging.[16,17]

Study of enantiospecific surface chemistry requires the adsorption of a chiral probe molecule onto a chiral surface and the use of a measurement that will detect the differences in the interactions of the two probe enantiomers with the two enantiomers of the surface. There are several types of enantioselectivity that have been observed by studies of the surface chemistry of chiral probe molecules on chirally modified surfaces. Tysoe and co-workers have used propylene oxide (PO) as a chiral probe molecule to investigate the enantioselectivity of Pd(111) surfaces modified by a variety of chiral adsorbates including *R*- and *S*-2-butanol.[17−20] For a given exposure of *R*- or *S*-PO to the chirally modified Pd(111) surface, the resulting coverages of adsorbed *R*- or *S*-PO are enantiospecific. Complementing the work on chirally modified surfaces is a body of work studying the enantiospecific adsorption of chiral probe molecules on naturally chiral surfaces.[1] The first experimental observation of enantiospecific chemistry on naturally chiral surfaces was made by Attard et al. while studying the electro-oxidation of D- and L-glucose on the $Pt(643)^{R\&S}$ surfaces.[21] They found that the $Pt(643)^S$ surface exhibited a greater reactivity with L-glucose than with D-glucose. Enantioselective behavior of chiral adsorbates on naturally chiral surfaces was also demonstrated by Gellman and co-workers with their temperature programmed desorption (TPD) studies of *R*- and *S*-propylene oxide and *R*-3-methylcyclohexanone on the $Cu(643)^{R\&S}$ surfaces.[22−24] These studies revealed differences in adsorption energies on the $Cu(643)^{R\&S}$ surfaces, providing a direct illustration of the enantiospecific properties of naturally chiral metal surfaces. More recently, the adsorption of D- and L-cysteine on a chiral $Au(17,11,9)^S$ surface was studied using X-ray photoelectron spectroscopy (XPS) and revealed enantiospecific core level binding energies in the amino and in the thiol group.[25] Held et al. also reported enantiospecific adsorption of alanine on chiral $Cu(531)^{R\&S}$ surfaces using XPS, low-energy electron diffraction (LEED), and near edge X-ray absorption fine structure spectroscopy (NEXAFS).[26]

Amino acids have long been identified as potentially useful chiral modifiers for catalytic surfaces. They possess two main functional groups (a carboxylic acid group (COOH) and an amine group (NH_2)), either one or both of which could contribute to the bonding to metal surfaces. Some amino acids have reactive side chains (e.g., the thiol group (−SH) in cysteine and the additional amine group in lysine) which could also be involved in their bonding to surfaces. Several research groups conducted infrared reflection absorption spectroscopy (IRAS) and XPS experiments under ultrahigh vacuum conditions to study the adsorbed state of glycine, alanine, proline, and other amino acids on single crystal Cu surfaces.[27,28] These amino acids were always found to be in their anionic, deprotonated form when adsorbed on the Cu surface. Moreover, under certain conditions, these amino acids were found to self-assemble into ordered superstructures held together by networks of intermolecular hydrogen bonds. Some of these ordered phases possess chirality which can be sustained wide domains on the surface.[11,27,28] In some cases, amino acids can induce reconstruction of achiral Cu surfaces by promoting step bunching and formation of high Miller index facets with kink structures that are naturally chiral.[7−9]

One of the most interesting chirally modified surfaces is the L-lysine modified Cu(100) surface used in this work. The adsorption of L-lysine on the Cu(100) surface was studied with scanning tunneling microscopy (STM).[7−9] After annealing at 430 K, a high coverage of L-lysine formed a (4 1, −2 4) overlayer structure. During annealing, monatomic steps on the surface bunch together to form chiral (3,1,17) facets. On the Cu(100) surfaces, there are eight possible (3,1,17) chiral facets with structures related by reflection and rotation symmetry: four of *R*-chirality and four of *S*-chirality. Zhao et al.[7−9] found only the four (3,1,17) facets with *R*-chirality, indicating that the L-lysine had imprinted its chirality onto the achiral Cu(100) surface. Recently, we have studied the adsorption energetics of D- and L-lysine on Cu(100) and $Cu(3,1,17)^{R\&S}$ and shown that they are consistent with the observations of enantiospecific chiral imprinting by Zhao et al.[2,7−9] The D- and L-lysine adsorption energies on $Cu(3,1,17)^{R\&S}$ exhibit diastereomerism, with L-lysine having a higher adsorption energy on the $Cu(3,1,17)^R$ surface than on the $Cu(3,1,17)^S$ surface. These observations suggest that chiral imprinting by chiral adsorbates could serve as a route to the production of naturally chiral metal surfaces.

In this work, we have used TPD to probe the enantiospecificity of *R*- and *S*-PO adsorption on lysine modified Cu(100). Enantiomerically pure *R*- or *S*-PO was adsorbed onto the D- or L-lysine modified Cu(100) surface using a range of both probe and modifier coverages. Titration using ^{13}CO was used to quantify the coverage of empty sites, θ_O, on the surface after lysine adsorption. *R*- and *S*-PO TPD measurements reveal enantiospecific peak desorption temperatures when the empty site density is in the range $\theta_O = 0-0.5$ monolayer (where 1 ML is defined as the density of Cu atoms in the Cu(100) surface). These exhibit true diastereomersim on the D- and L-lysine modified Cu(100) surfaces. The enantiospecific difference in the PO peak desorption temperatures is 5.5 K at $\theta_O \approx 0.25$ and corresponds to an enantiospecific desorption energy difference of ∼2 kJ/mol. This result is in stark contrast to our previous failure to observe enantiospecific adsorption of either PO or *R*-3-methylcyclohexanone on Cu(100) and Cu(111) surfaces modified with a variety of chiral species including 2-butanol, 2-butanoxy, alanine, and alaninol.[16] We suggest that the potential for hydrogen bonding between the lysine modifier and the PO probe is a key difference that might account for the enantiospecific adsorption observed in this work.

2. EXPERIMENTAL SECTION

The experiments were performed in a stainless steel ultrahigh vacuum (UHV) chamber with a base pressure of 2×10^{-10} Torr. The chamber is equipped with a quadrupole mass spectrometer used for TPD measurements, an ion sputter gun to clean the sample by Ar^+ bombardment, leak valves to admit gases into the chamber, an evaporative source to sublime amino acids in vacuo, and low energy electron diffraction (LEED) optics to study the structure of clean surfaces and adsorbate overlayers.

The Cu(100) single crystal disk of approximately 1 cm diameter was used as a substrate for adsorption of the lysine modifier followed by

dx.doi.org/10.1021/la3027557 | Langmuir 2012, 28, 15251−15262

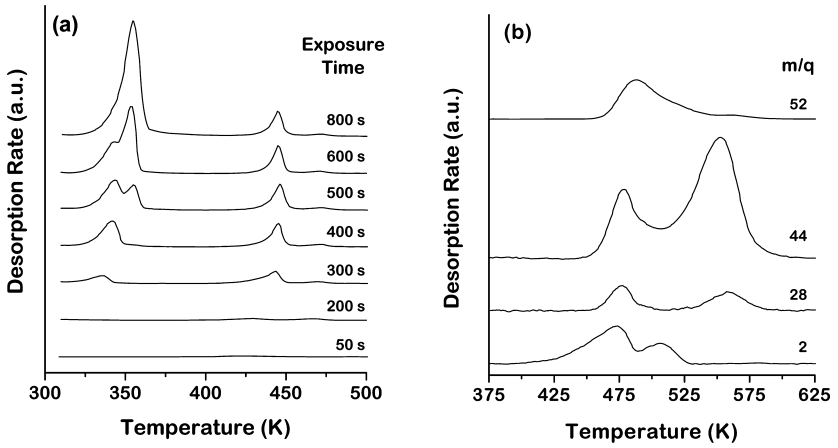

Figure 1. TPD spectra for L-lysine on Cu(100). (a) Temperature programmed desorption (TPD) spectra of L-lysine from the Cu(100) surface following increasing L-lysine exposure times of 50, 200, 300, 400, 500, 600, and 800 s. The signals at were monitored at m/q = 30, and the heating rate was 1 K/s. Four peaks are present in the TPD spectra obtained following exposures > 500 s: desorption of L-lysine from step defects (~470 K), first-layer desorption (~445 K), and multilayer desorption (345, 360 K) from the Cu(100) terrace. (b) TPD spectra following exposure of Cu(100) to L-lysine for 50 s obtained by monitoring the signals at m/q = 2, 28, 44, 52. No desorption of intact lysine at m/q = 30 was detected in the TPD experiment. Curves are offset for clarity.

coadsorption of enantiomerically pure PO or ^{13}CO. Only one side of the Cu(100) sample was used in the adsorption studies. The Cu(100) sample was spot-welded between two Ta wires mounted to a sample holder at the bottom of a manipulator. The sample could be resistively heated to >1000 K and cooled to <100 K using liquid-nitrogen. The sample temperature was measured with a chromel-alumel thermocouple spot-welded to the edge of the Cu(100) sample via a thin strip of Ni foil. During heating and cooling, the sample temperature was controlled by a computer.

L- and D-Lysine (Sigma-Aldrich, $NH_2(CH_2)_4-CH(NH_2)-COOH$, ≥98% purity) were deposited onto the Cu(100) surface by sublimation from an evaporative source consisting of lysine in a glass vial which was heated resistively by nichrome wire. The dosing is performed with a direct line of sight between the source and the Cu(100) surface. Prior to the dosing the glass vial was heated for roughly 1 h to reach a steady state temperature. The deposition rate was controlled by the sublimation temperature which was measured and controlled using a chromel-alumel thermocouple connected to a digital PID-temperature controller (Micromega). The real exposure of the Cu(100) sample to lysine vapor could not be determined based on measurements of changes in the background pressure in the UHV chamber. Instead exposures are reported in terms of exposure time, i.e. the period of time that the Cu(100) sample was exposed to the lysine vapor emerged from the evaporative source held at 373 K. This exposure time is controlled by opening and closing of a shutter placed in front of the evaporative source.

PO vapors were introduced into the UHV chamber through a leak valve. Enantiomerically pure and racemic PO (Alfa Aesar, C_3H_6O, 99%) were first transferred to clean glass vials and subjected to multiple freeze−pump−thaw cycles to remove air, water vapor, and other high vapor pressure impurities. The purity of the chemical was verified by mass spectrometry before use. Exposures are reported in units of Langmuirs (L) where 1 L = 10^{-6} Torr·s.

Isotopically labeled ^{13}CO gas (Isotec, 99 atom % ^{13}C, <5 atom % ^{18}O) and Ar gas (Matheson, 99.995% purity) were taken from high pressure lecture bottles and were also introduced into the vacuum chamber via leak valves. The purity of each gas was verified by mass spectrometry before use. The ^{13}CO was used to estimate the coverage of bare surface sites on Cu(100) surfaces modified by submonolayer coverages of adsorbed lysine. This ^{13}CO titration method was previously employed elsewhere to estimate the coverage of adsorbed amino acids, for example, glycine, alanine, and proline, on the Pd(111) surface.[29−31]

The Cu(100) surface was cleaned by repeated cycles of 1 keV Ar^+ ion sputtering while annealing at 750 K for 500 s. The sample was then cooled at a controlled rate of −1 K/s, until the clean surface yielded a sharp LEED pattern. Following the adsorption of lysine and annealing to the desired temperature, the overlayer structure was determined using LEED. TPD was used to study the adsorption and desorption of lysine on Cu(100) and to study the coadsorption of ^{13}CO, racemic PO, *R*-PO, or *S*-PO with D- or L-lysine on the Cu(100) surfaces. Following adsorption of the desired compound(s) at an appropriate adsorption temperature, the sample was positioned in front of the aperture to a quadrupole mass spectrometer used for TPD measurements. TPD spectra were obtained by heating the Cu(100) surface at a constant rate while using the quadrupole mass spectrometer to monitor the rate of desorption of various species from the surface. The heating rate was 1 K/s unless otherwise specified.

3. RESULTS

3.1. Adsorption of Lysine on Cu(100). *3.1.1. TPD Spectra of Lysine from Cu(100).* Prior to studying enantiospecific adsorption on Cu(100) modified with lysine, it was necessary to characterize the adsorption and surface chemistry of the lysine modifier alone on the clean achiral Cu(100) surface. The desorption and decomposition of L-lysine on the Cu(100) surface were studied by TPD and LEED. The clean Cu(100) surface was initially held at 300 K and then exposed to L-lysine vapor sublimed at 373 K. The signals at various mass-to-charge ratios (m/q = 2, 28, 30, 44, 52, 56, 67, 84) were monitored with the mass spectrometer while the sample was heated at 1 K/s. Figure 1a displays the TPD spectra recorded by monitoring the signal at m/q = 30 (the most intense signal in the L-lysine fragmentation pattern) following increasing exposures of the Cu(100) surface to L-lysine. For L-lysine exposures of <150 s, there is no evidence of molecular desorption from the surface. Starting at an exposure of ~200 s, an L-lysine desorption feature appears at 430 K. The peak saturates at an exposure of about 400 s having shifted to a peak temperature of approximately 445 K. This desorption feature has the fragmentation pattern of molecular L-lysine and is attributed to molecular desorption from the first-layer.

Desorption peaks at temperatures of 345 and 360 K were also observed in the signal at m/q = 30 following L-lysine exposures > 200 s. Both of these peaks have fragmentation patterns matching that of L-lysine and are attributed to

dx.doi.org/10.1021/la3027557 | *Langmuir* 2012, 28, 15251−15262

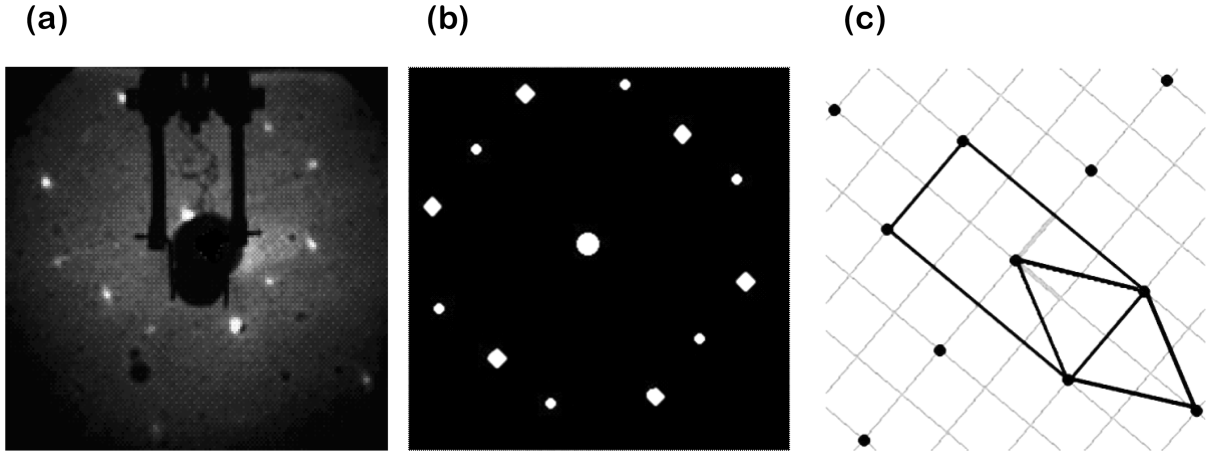

Figure 2. c(2 × 4) phase of the L-lysine on Cu(100). (a) LEED pattern at 3 eV of the c(2 × 4) L-lysine overlayer on the Cu(100) surface obtained after annealing the saturated monolayer at 430 K for 20 min. (b) Schemtic representation of the LEED pattern in (a). "●" denotes the (0,0) spot while "◆" and "•" are the overlayer diffractions spots for two domains. (c) The real space lattice corresponding one domain of the LEED pattern in (a) and the reciprocal lattice in (b).

desorption of molecular L-lysine from adsorbed multilayers. The interesting characteristic of the desorption peak at 345 K is that it grows and saturates concurrently with the first-layer desorption peak at 445 K. This suggests that L-lysine adsorbs on the Cu(100) surface in a bilayer structure even at submonolayer coverages. The peak at 360 K appears at exposures ≥500 s and does not saturate with increasing exposure. This peak at 360 K is attributed to sublimation of bulk-like multilayer L-lysine. The appearance of a 345 K L-lysine desorption feature at temperatures below that of the bulk-like L-lysine multilayer is quite unusual.

There is a small, high temperature peak at ∼470 K in the TPD spectra of L-lysine from Cu(100) shown in Figure 1a. Recently published work has shown that this feature occurs at the same temperature as the desorption of L-lysine from the $Cu(3,1,17)^R$ surface.[2] Hence, this feature on the Cu(100) surface is attributed to the desorption of L-lysine from step defects on the Cu(100) surface.

No molecular L-lysine desorption was observed at exposures <200 s (Figure 1a), suggesting that at low coverages most L-lysine must adsorb irreversibly on the Cu(100) surface and undergo decomposition during heating. Figure 1b shows the TPD spectra recorded using signals at m/q = 2, 28, 44, 52 following exposure of Cu(100) to L-lysine for 50 s. These TPD profiles show complex behavior at temperatures above the first-layer desorption temperature of 445 K, indicating that at low coverage adsorbed L-lysine undergoes a series of thermal decomposition reactions during heating to generate decomposition products including H_2 and CO_2. Even at the highest exposure when bulk multilayers of lysine have formed, a fraction of the adsorbed lysine undergoes decomposition while the remainder desorbs molecularly during heating. A number of decomposition products have been identified on the basis of a TPD experiment in which all m/q ratios from 1 to 150 were monitored during L-lysine decomposition on Cu(100) following an exposure of 500 s. That experiment resulted in the detection of a number of species desorbing from the surface in the temperature range 450 − 600 K. These included: NH_3 (m/q = 17), H_2 (m/q = 2), C_4H_4 and/or C_2N_2 (m/q = 52), C_2H_4, CO and/or N_2 (m/q = 28), CO_2 (m/q = 44), HCN (m/q = 27) and H_2O (m/q = 18). These decomposition products are generally consistent with the observations of thermal decomposition of other amino acids, for example, glycine, alanine, and proline, on other metal surfaces.[29−32]

TPD experiments were also performed for a range of D-lysine coverages on the Cu(100) surface. Desorption of L- and D-lysine from Cu(100) should not be enantiospecific because an achiral surface should not distinguish the two enantiomers. Indeed, TPD spectra for D-lysine on Cu(100) were not significantly different from those acquired under the same conditions for L-lysine on the Cu(100) surface.

3.1.2. LEED from L-Lysine on Cu(100). The ordering of the L-lysine overlayer on Cu(100) was studied using LEED. L-lysine was sublimed from the evaporative doser at 373 K while the Cu(100) surface was held at 300 K. Following exposure to L-lysine for 400−600 s to saturate the adsorbed monolayer, the surface was annealed at 430 K for 20 min. The LEED experiments used a low beam energy of 33 eV because amino acid overlayers are very sensitive to electron beam damage. Figure 2a shows the LEED pattern obtained from the L-lysine overlayer. The diffraction spots in this LEED pattern match those shown in Figure 2b which displays the reciprocal lattice of a c(2 × 4) overlayer with two domains. The corresponding c(2 × 4) real space lattice is illustrated in Figure 2c. The formation of a c(2 × 4) overlayer has also been reported for the adsorption of other amino acids, e.g. glycine, alanine, phenylalanine, on the Cu(100) surface.[9]

Now the question is, what adsorption geometry of lysine would be allowed in this c(2 × 4) unit cell? The c(2 × 4) unit cell has dimensions of 5.11 Å × 10.22 Å and the length of lysine is ∼13 Å.[7,33] The rhombohedral primitive unit cell also has long and short dimensions of 5.11 Å × 10.22 Å but half the area of the c(2 × 4) unit cell. Hence, contrary to the adsorption model proposed by Zhao et al.,[7] it is unlikely that the primitive unit cell would allow bonding via both carboxylate O atoms and the amino N atoms at either end of the adsorbed lysine molecules. In order to allow an amino acid such as lysine with a bulky side group to adopt a c(2 × 4) overlayer structure, it is likely that the side chain is tilted away from the surface and that the amino N atom in the side group is not involved in bonding to the Cu(100) surface. This is consistent with the adsorption geometry proposed in a previous study of lysine on Cu(110).[34]

3.2. Estimation of Empty Site Density on Lysine Modified Cu(100). ^{13}CO adsorption has been used to quantify

dx.doi.org/10.1021/la3027557 | *Langmuir* 2012, 28, 15251−15262

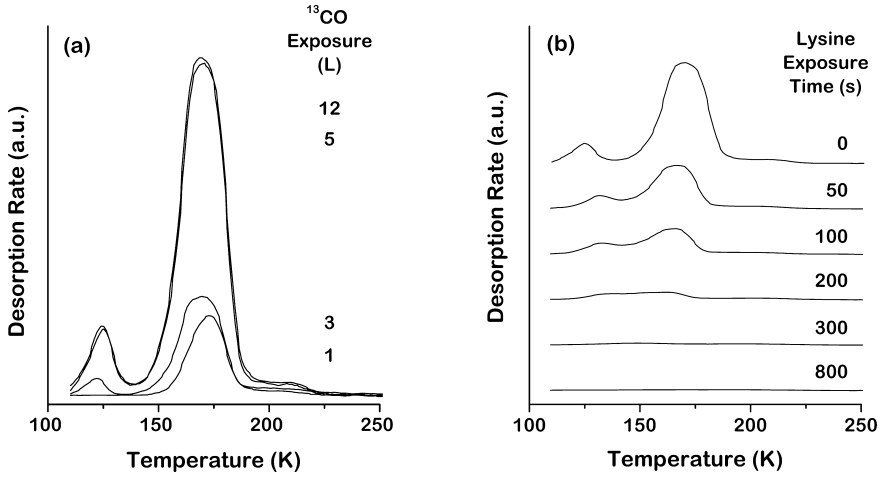

Figure 3. TPD spectra of ^{13}CO. (a) TPD spectra of ^{13}CO from clean Cu(100) following various ^{13}CO exposures with the surface at 95 K. The Cu(100) surface is saturated following an exposure of 5 L. (b) TPD spectra of ^{13}CO from the D-lysine modified Cu(100) surface acquired after D-lysine exposure times of 0 − 800 s with the surface at 300 K followed by a 5 L ^{13}CO exposure with the surface at 95 K. The coverage of ^{13}CO on Cu(100) decreases with increasing D-lysine exposures, and desorption of ^{13}CO was nearly undetectable for lysine exposure times higher than 300 s. TPD spectra were collected while heating the surface at 1 K/s and monitoring the signal at m/q = 29. Curves are offset for clarity.

the empty site coverage, θ_O, on the Cu(100) surface following L-lysine adsorption. Determination of the exposed surface coverage through titration by ^{13}CO is particularly important for quantification of enantiospecific adsorption of the chiral probes on the L-lysine modified surface. Adsorption of chiral probes will require the availability of empty sites, if the probe is to interact with the Cu surface. L-lysine coverage cannot be determined directly from L-lysine desorption measurements because, as mentioned previously, L-lysine adsorbs into the second layer at 300 K before completion of the first layer. In addition, a fraction of the adsorbed L-lysine decomposes during the TPD experiments. The ^{13}CO titration method has been used successfully in studies of glycine, alanine, and proline adsorption on the Pd(111) surface.[29−31] Isotopically labeled ^{13}CO was used because it can be distinguished using mass spectrometry from the ^{12}CO formed by thermal decomposition of L-lysine.

Adsorption of ^{13}CO was first studied on clean Cu(100) in order to find the ^{13}CO exposure needed to saturate the surface. ^{13}CO was admitted into the vacuum chamber through a leak valve while the adsorption took place on the surface at 95 K. The surface was then heated at 1 K/s to collect desorption spectra. Figure 3a displays the TPD spectra of ^{13}CO from clean Cu(100) recorded at increasing ^{13}CO exposures. After the highest exposure, three desorption features are visible in Figure 3a; peaks at 125 K and at 168 K as well as a small shoulder at 205 K. It is known that CO adsorbs at the atop sites to form a c(2 × 2) overlayer on Cu(100);[35−39] hence, the major desorption peak at 168 K is attributed to desorption of CO from the atop sites. At higher coverages, a small desorption peak at 125 K starts to develop. The small shoulder at ∼205 K is assigned to ^{13}CO desorption from the step defects on the surface because the intensity of this feature relative to the lower temperature features is significantly increased when ^{13}CO is adsorbed on the high Miller index Cu(3,1,17) surface having chiral kinked steps. As the CO multilayer is known to form only at temperatures below 30 K,[40] that is, much lower than the adsorption temperature used in these experiments, multilayer desorption of CO would not be seen in the TPD spectra in Figure 3a. Perhaps the most useful information obtained from Figure 3a is that an exposure of 5 L is sufficient to saturate the Cu(100) surface with ^{13}CO at a total coverage of θ_{CO} = 0.5 relative to the Cu(100) atomic density.[35−39] Hence, Cu(100) surfaces modified by submonolayer coverages of L-lysine were exposed to 5 L of ^{13}CO in order to titrate the empty surface.

After exposing the Cu(100) surface to L- or D-lysine for a desired period of time at 300 K, the surface was cooled to <95 K to allow exposure to 5 L of ^{13}CO. The ^{13}CO desorption spectra from the Cu(100) surface modified by various D-lysine exposures are shown in Figure 3b. As expected, the coverage of ^{13}CO decreases with increasing D-lysine exposure. At a D-lysine exposure of 300 s, the signal intensity for ^{13}CO becomes nearly undetectable as the Cu(100) surface is fully saturated with lysine. Note that the complete blocking of ^{13}CO adsorption by L-lysine occurs at an L-lysine exposure of ∼400 s, identical to that at which the L-lysine monolayer desorption features at 445 and 345 K become saturated (Figure 1a).

3.3. Enantioselective Adsorption of PO on Lysine Modified Cu(100). *3.3.1. Adsorption of PO on Clean Cu(100).* Before using PO as a probe of enantiospecific adsorption on the lysine modified Cu(100) surface, adsorption and desorption of PO was studied on the clean Cu(100) surface. Figure 4 shows the TPD spectra of PO from clean Cu(100) recorded after increasing exposures of the surface to racemic PO. The surface was held at 95 K during exposures to racemic PO ranging from 0.1 to 1.2 L. PO adsorbs reversibly on the clean Cu(100) surface and desorbs molecularly during heating without any detectable decomposition. The TPD spectra of PO on clean Cu(100) shown in Figure 4 reveal the desorption of PO from Cu(100). At low coverages, desorption occurs at 180 K and shifts to 152 K once the monolayer is saturated. This is indicative of repulsive interaction between the adsorbed PO molecules. Following an exposure of ∼0.5 L, the clean Cu(100) surface is covered with a saturated monolayer of PO. After exposures > 0.5 L, multilayer desorption of PO is observed at approximately 121 K. These TPD spectra obtained from the clean Cu(100) surface will be used as baseline measurements to determine the effect of preadsorbed lysine on the coverages of PO and on the kinetics of PO desorption when lysine and PO are coadsorbed on the surface. The fact that PO

dx.doi.org/10.1021/la3027557 | Langmuir 2012, 28, 15251−15262

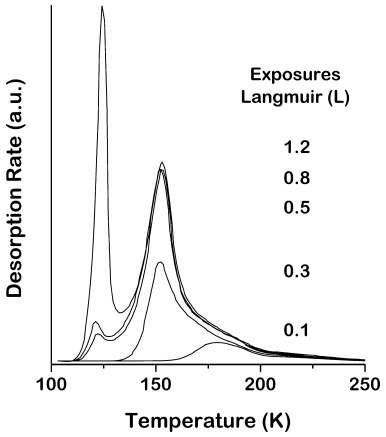

Figure 4. TPD spectra of racemic PO from clean Cu(100) following PO exposures of 0.1−1.2 L with the surface at 95 K. The high temperature peak (152 K) corresponds to monolayer desorption from the Cu(100) surface, while the low temperature peak (121 K) corresponds to multilayer desorption. TPD spectra were collected while heating the surface at 1 K/s and monitoring the signal at m/q = 58.

desorbs from the Cu(100) surface at temperatures well below the temperatures at which the first layer of adsorbed lysine either desorbs or decomposes (>300 K) means that PO can be desorbed from a lysine modified Cu(100) surface multiple times without the need to recreate the lysine modifier layer between each PO desorption measurement.

3.3.2. Adsorption of PO on Lysine Modified Cu(100). The desorption kinetics of *S*- and *R*-PO from the D- or L-lysine modified Cu(100) surface were studied in order to reveal enantiospecific behavior. The Cu(100) surface was modified with different initial coverages of D- or L-lysine. With the Cu(100) sample held at 300 K and the lysine powder at 373 K, the surface was exposed to D- or L-lysine vapor for 50, 100, 150, 175, 200, or 225 s. Each of these chirally modified surfaces was then cooled to 95 K to allow subsequent adsorption of *R*- or *S*-PO, followed by a TPD experiment to detect desorption of PO. At 95 K, PO will adsorb both on the exposed Cu(100) sites and as a multilayer on the lysine modifier. We are interested in the adsorption of PO on the bare Cu(100) surface, but in the presence of the lysine modifier, as indicated by desorption at temperatures >140 K. The available sites for adsorption of PO onto the Cu(100) surface are reduced as the initial coverage of lysine modifier is increased. Hence, for each increased lysine exposure, the PO exposure was decreased such that the coverage of the PO adsorbed on the Cu(100) was saturated but its desorption peak was not overwhelmed by the signal from the desorption of the PO multilayer on the lysine layer.

TPD spectra were acquired for both *R*- and *S*-PO on the Cu(100) surface modified by various coverages of D- or L-lysine modifier. Figure 5 presents the TPD spectra of *R*- and *S*-PO from the Cu(100) surface modified with increasing L-lysine coverages. Figure 5A shows the TPD spectra of *R*- and *S*-PO from the Cu(100) surface modified by the lowest L-lysine exposure of 50 s (equivalent to $\theta_O \approx 0.63$ ML based on the ^{13}CO titration method). The surface was exposed to 1.5 L of *R*-

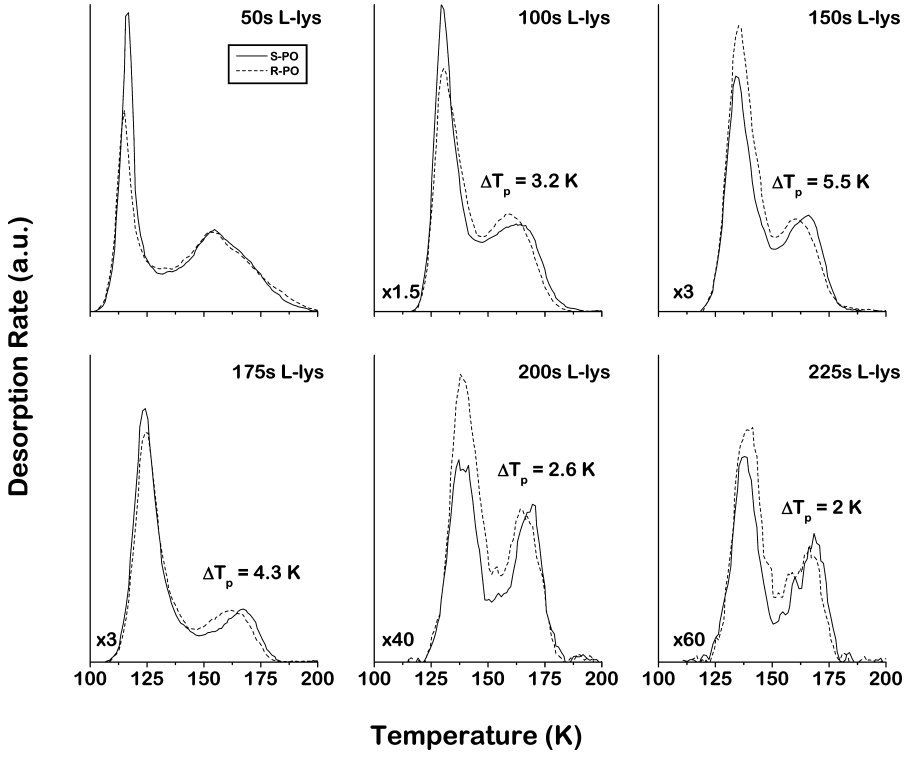

Figure 5. TPD spectra of *S*- and *R*-PO from the Cu(100) surface modified by L-lysine exposures of (a) 50 s, (b) 100 s, (c) 150 s, (d) 175 s, (e) 200 s, and (f) 225 s with the surface at 300 K. PO was then exposed to the surface at 95 K. The PO exposures were 1.5, 1.0, 0.25, 0.1, 0.006 to 0.005 L in (a)−(f), respectively, such that the peak due to PO adsorbed to the Cu(100) surface was not overwhelmed by the signal of the multilayer desorption peak. *S*-PO was found to adsorb more strongly than *R*-PO (desorb at a higher temperature) on the L-lysine modified Cu(100) surface. The enantiospecific desorption was observed over a narrow range of L-lysine exposures with maximum peak temperature difference occurring after a L-lysine exposure time of 150 s. A heating rate of 1 K/s was used and the signal at m/q = 58 was monitored.

dx.doi.org/10.1021/la3027557 | *Langmuir* 2012, 28, 15251−15262

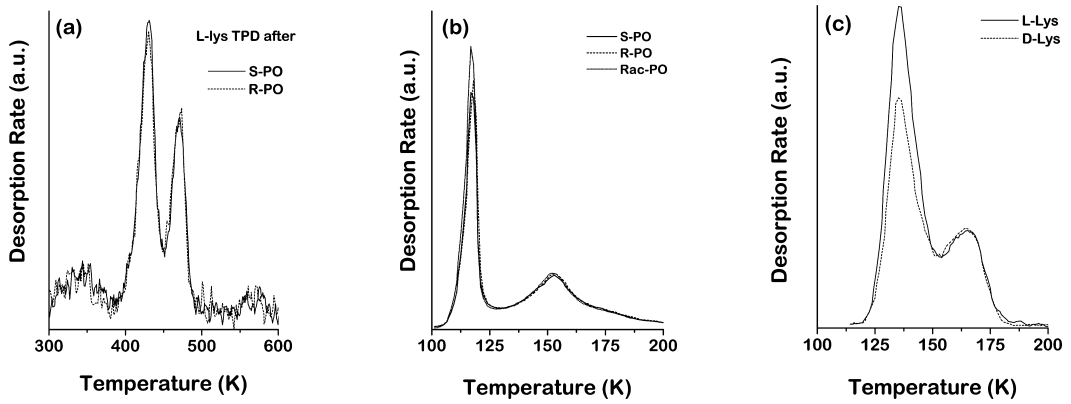

Figure 6. Reproducibility and control experiments. (a) TPD of L-lysine recorded following exposure to L-lysine for 150 s at 300 K and an *S*- or *R*-PO exposure of 0.25 L at 95 K. The two overlapping TPD traces reveal identical amounts of L-lysine adsorbed on the surface before adsorption of *S*-PO and *R*-PO in separate experiments. TPD measurements were performed at a heating rate of 1 K/s while monitoring the signal at $m/q = 30$. (b) TPD of *S*- PO, *R*-PO and racemic PO from the clean Cu(100) surface following PO exposures of 2 L. As expected for desorption from an achiral surface, the three overlapping TPD traces have identical monolayer peak desorption temperatures at ∼152 K. (c) TPD of racemic PO from the Cu(100) surface modified by exposure to L- or D-lysine for 150 s at 300 K following a rac-PO exposure of 0.25 L at 95 K. As expected for desorption of a racemic mixture with no net chirality, these two TPD traces reveal almost identical monolayer peak desorption temperatures of 164 K. TPD spectra were collected at a heating rate of 1 K/s while monitoring the signal at $m/q = 58$.

or *S*-PO and then heated at 1 K/s to obtain the TPD spectra. The TPD spectra of *R*- and *S*-PO were found to be qualitatively similar to those obtained from the clean Cu(100) surface, as shown in Figure 4. The multilayer peak desorbs at 121 K and the monolayer desorbs over the range 140−190 K. There are no observable differences between the desorption features of the *R*- and the *S*-PO. The differences in the amplitudes of the multilayer peaks are attributed to differences in multilayer coverage arising from small differences in the PO exposure. We are concerned only with the monolayer desorption features which are highly reproducible because the PO exposure is sufficient to saturate the available empty sites on the Cu(100) surface. Investigations of the enantiospecific desorption of *R*- and *S*-PO were performed with an L-lysine exposure time of 100 s, resulting in an empty site coverage of $\theta_O \approx 0.40$ ML. Figure 5b shows the PO TPD spectra obtained after exposing this L-lysine modified surface to 1 L of *R*- or *S*-PO. The *S*-PO monolayer was observed to desorb at a temperature that was $\Delta T_p = 3.2$ K higher than the *R*-PO monolayer. Increasing the L-lysine exposure time to 150 s ($\theta_O \approx 0.25$ ML) further enhances the difference in the desorption kinetics of *R*- and *S*-PO. The TPD spectra shown in Figure 5c collected after a PO exposure of 0.25 L revealed a peak desorption temperature difference of $\Delta T_p = 5.5$ K. This was the largest peak desorption temperature difference obtained for *R*- and *S*-PO desorption from the L-lysine modified Cu(100) surface. Further increasing the L-lysine exposure times to 175, 200, and 225 s resulted in the values of ΔT_p decreasing to 4.3 K, 2.6, and 2 K, respectively (Figure 5d−f). Note that, as the coverage of L-lysine on the Cu(100) surface increases, the coverage of empty sites at which the PO monolayer can adsorb decreases until the monolayer desorption peak becomes so small that it is impossible to measure ΔT_p accurately.

While coadsorption of lysine and PO on the Cu(100) surface did not qualitatively affect the desorption features of PO, the monolayer peak desorption temperature of PO appeared to be higher with the lysine modifier on the surface than without. As seen in Figure 5, the monolayer desorption peaks of both *S*- and *R*-PO shift to higher temperature (from 154 to 168 K) with increasing lysine exposure. This indicates that interaction between coadsorbed PO and the lysine modifier in the first layer must be attractive, resulting in a higher desorption energy of PO than from the clean Cu(100) surface. In fact, this interaction between PO and lysine modifier is not limited to the first layer. The desorption peaks at 135 K in Figure 5b, c, e, f were attributed to desorption of PO molecules on top of the lysine modifiers. These PO molecules desorb at temperatures higher than the PO multilayer desorption temperature (121 K) but lower than the monolayer desorption temperature (154 to 168 K). More importantly, the multilayer peak desorption temperature shift from 130 to 138 K with increasing lysine exposure indicating that there are attractive interactions between PO in the second layer and the lysine modifier layer.

In order to demonstrate that the *R*- and *S*-PO desorption peak shifts shown in Figure 5 arise from enantiospecificity, it is necessary to demonstrate the same, but opposite peak shifts on the Cu(100) surface modified by D-lysine. PO TPD experiments were performed on the D-lysine modified Cu(100) surface under the same conditions as used for the experiments on L-lysine modified Cu(100) shown in Figure 5. When using D-lysine modified Cu(100), *R*-PO has a higher desorption temperature than *S*-PO, opposite to the observations on the L-lysine modified Cu(100) surface. Thus, *R*- and *S*-PO desorption from Cu(100) surface modified by D- and L-lysine exhibits true diastereomerism and must arise from enantiospecific adsorbate-modifier interactions.

As sputtering was performed between the experiments with different lysine coverages (Figure 5) and a new layer of D- or L-lysine was adsorbed on the surface, it is important to verify that the same amount of D- or L-lysine modifier was present on the surface during adsorption of *S*-PO and *R*-PO for a particular lysine exposure. A TPD spectrum of the adsorbed lysine was obtained after each experiment adsorbing and desorbing *S*- or *R*-PO. To demonstrate the reproducibility of the lysine coverage, Figure 6a shows the TPD spectra of L-lysine obtained following exposure to L-lysine for 150 s and an *R*- or *S*-PO exposure of 0.25 L. Figure 6a is identical (but greatly magnified) to the desorption peaks of lysine at low exposure (<200 s) in Figure 1. As explained earlier, the two peaks at ∼430 and 470 K in Figure 6a are attributed to lysine desorption

dx.doi.org/10.1021/la3027557 | *Langmuir* 2012, 28, 15251−15262

from the first layer on the Cu(100) surface and from step defects, respectively. Most importantly, in Figure 6a, the two overlapping TPD traces indicate that identical amounts of L-lysine were present on the surface before and after each of the *S*-PO and *R*-PO desorption experiments.

To verify that the observed difference between *R*- and *S*-PO desorption from the lysine modified Cu(100) surface is truly enantiospecific, several control experiments must be performed. First, desorption of both enantiomers of PO from the achiral Cu(100) surface must be shown to be identical. Figure 6b indicates that the monolayer peak desorption temperatures for *S*-, *R*-, and racemic PO from the achiral Cu(100) surface are identical, as expected for desorption from an achiral surface. The three overlapping TPD traces in Figure 6b also verify the reproducibility of the desorption measurements. As a second control experiment, desorption of racemic PO from Cu(100) modified by L- or D-lysine exposure for 150 s was studied. Figure 6c shows that the racemic PO desorption peak on both the L- and D-lysine modified Cu(100) surfaces occurs as 164 K and with the same peak shapes. As expected, this control experiment does not reveal any enantiospecificity. This experiment does indicate the accuracy with which peak desorption temperatures can be reproduced.

The results and controls detailed above clearly demonstrate that enantiomerically pure *R*- and *S*-PO adsorbs enantiospecifically on Cu(100) surfaces that have been chirally modified with D- or L-lysine. The observed diasteroemerism and the careful control experiments, all indicate that this is a truly enantiospecific phenomenon.

4. DISCUSSION

4.1. Morphology of Lysine on Cu(100). Before considering the enantiospecific adsorption of PO on lysine modified Cu(100), we discuss the surface chemistry of the lysine modifier. One of the complicating features is the fact that lysine appears to adsorb into three phases that are kinetically distinct with respect to desorption. The *monolayer* phase undergoes both decomposition and desorption during heating (Figure 1). When the total coverage of lysine is low, it is adsorbed in the monolayer phase and decomposes at temperatures > 450 K. At higher coverages, a fraction of the monolayer phase desorbs molecularly during heating at temperatures in the range 430−445 K. What is surprising is that the onset of desorption from the monolayer is also accompanied by desorption at 345 K of a phase that we refer to as the *capping* layer. The amount of lysine desorbing from the capping phase is roughly equal to the amount that can desorb from the monolayer phase. The details of the nature of the capping phase are not known and are not the subject of this work. However, one can conclude that the capping layer is kinetically distinct from the monolayer phase that desorbs at 430 K. What is even more surprising is that the capping layer persists even after the total coverage has reached the point that *multilayer* desorption is apparent at 360 K. In Figure 7, we have attempted to illustrate how the fractional coverage of lysine develops in each phase with increasing total coverage of lysine. Figure 8 illustrates a proposed molecular picture of the development of the lysine modifier layer that is consistent with the observations from TPD at various coverages. For lysine coverages < 0.5 ML, generated by exposures below ~200 s, lysine in the monolayer is irreversibly adsorbed directly on the Cu(100) surface. Heating results in the complete decomposition of this layer, as indicated by the TPD spectra

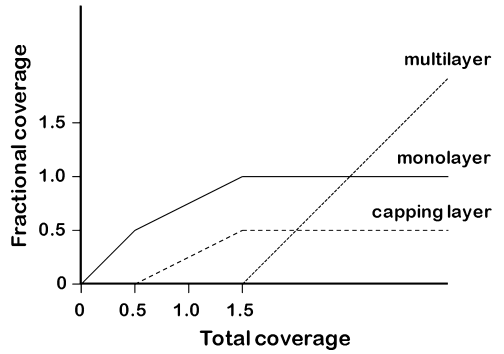

Figure 7. Proposed distribution of lysine coverages among different adsorption phases (i.e., first layer, capping layer, multilayer) as a function of the total coverage.

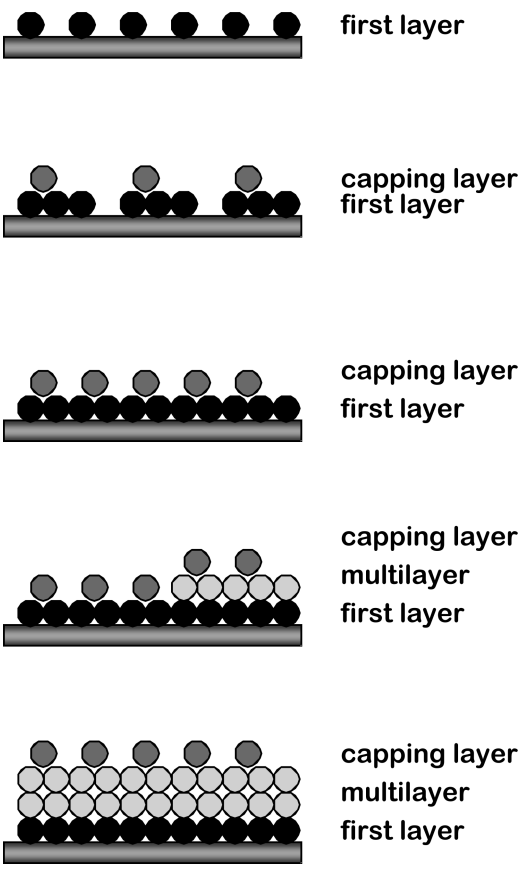

Figure 8. Schematic of the proposed arrangement of lysine molecules when adsorbed on the Cu(100) surface at various coverages. Gray circles represent the "capping" lysine molecules desorbing at ~345 K, open circles represent the bulklike crystalline multilayer phase desorbing at ~360 K, and the solid filled circles represent the first-layer lysine desorbing at ~445 K.

shown in Figure 1b. Increasing the lysine coverage to 0.5 ML < θ_{lys} < 1.5 ML causes lysine to start adsorbing into both the monolayer and the capping layer simultaneously, and hence small bilayer islands are formed. When coverage exceeds 1.5 ML, additional lysine adsorbs into the *multilayer* phase such that 3D islands form. This is supported by the appearance of the multilayer desorption peak at ~360 K which then grows indefinitely with increasing lysine exposure. At this point, the capping layer lysine persists and continues to desorb at 345 K. As seen in Figure 1a, heating such a lysine-covered Cu(100)

dx.doi.org/10.1021/la3027557 | *Langmuir* 2012, 28, 15251−15262

surface results in three desorption peaks at 345, 360, and 445 K. What remains a mystery is why the capping layer, which apparently has a lower desorption energy than either the monolayer or the multilayer, would be stable against conversion into either monolayer or multilayer.

A previous study of the multilayer growth of benzene on Ru(001) has reported similar structural arrangement of the topmost layer, and has provided spectroscopic evidence that the crystalline multilayer of benzene is always covered by an amorphous capping layer.[41] For such multilayer growth, this could mean that a direct transition from the crystalline multilayer phase to the vacuum is thermodynamically less favored than going through a crystalline−amorphous−vacuum interlayer arrangement.

One interesting finding from our LEED study was that the observed c(2 × 4) overlayer structure induced by high coverage of lysine on Cu(100) after annealing at 430 K did not match the previously reported STM results[7] which showed a (4 1, −2 4) overlayer structure on Cu(100) following high L-lysine exposure and annealing at 430 K. Despite our attempts, we were unable to find conditions for deposition or treatment of the L-lysine on Cu(100) that produced the (4 1, −2 4) structure. On the other hand, the c(2 × 4) unit cell has been observed for a number of other amino acids on Cu(100).[9]

From the STM results, it was suggested that the (4 1, −2 4) unit cell allows the bonding of L-lysine to Cu(100) through both carboxylate O atoms and both amino N atoms (one in the side chain and the other attached to the chiral carbon).[7] In contrast, our LEED results reveal a c(2 × 4) unit cell that could not accommodate the L-lysine molecule with its long side chain lying flat on the surface. If there is one lysine molecule per unit cell, then our reported c(2 × 4) unit cell gives an absolute coverage of 0.25 lysine molecules per Cu atom. Our proposal for L-lysine orientation in the first layer, based on the c(2 × 4) unit cell observed after annealing at 430 K, corresponds to adsorption with a closely packed upright stance rather than the flat-lying orientation suggested by Zhao et al.[7−9]

It is important to note that the conditions for forming the c(2 × 4) structure require annealing a high coverage of lysine at 430 K for an extended period of time. At the very least, this will result in the desorption of the capping layer described above. Given that the onset of the reversible desorption of the lysine monolayer occurs at ∼430 K, the annealing may induce additional transformations in the lysine adlayer. Our studies of enantiospecific lysine adsorption were conducted by coadsorbing PO onto adlayers of lysine adsorbed at 300 K. Hence, the relationship between the c(2 × 4) structure and the lysine adlayers on which we have observed enantiospecific adsorption of PO is not known.

4.2. Coverage Dependence of PO Adsorption on Lysine Modified Cu(100). Given the complexity of lysine adsorption on the Cu(100) surface and the apparent coexistence of monolayer and capping layer lysine species, defining a coverage of lysine based on the use of TPD experiments is probably not valuable. Even if this were attempted, the relationship between lysine coverage and the concentration of empty sites for PO adsorption would not be obvious. Instead we have titrated the lysine modified Cu(100) surface with ^{13}CO as a means of measuring the loss of empty adsorption sites as a function of lysine exposure to the surface. CO is known to form a c(2 × 2) layer with a coverage of θ_{CO} = 0.5 when adsorbed on Cu(100) at 300 K.[35−39] Figure 9 plots the saturation ^{13}CO yield (■) following adsorption at 95 K on

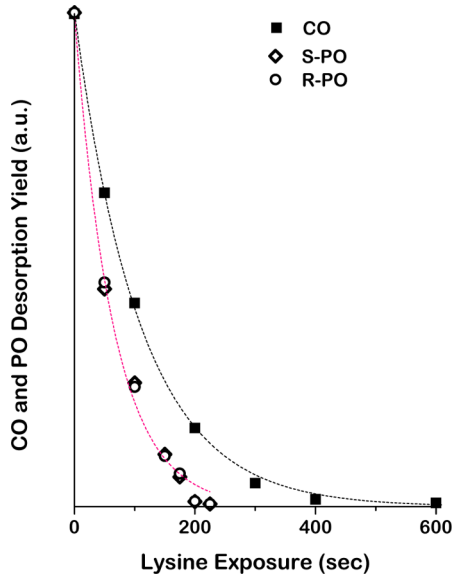

Figure 9. Desorption yields of ^{13}CO (m/q = 29, data from Figure 3) and *R*- and *S*-PO (m/q = 58, data from Figure 5) as a function of lysine exposure to the Cu(100) surface. Desorption yields were measured for ^{13}CO, *R*- and *S*-PO adsorbed in the monolayer to the Cu(100) surface and normalized for the clean Cu(100) surface with no lysine exposure. The smooth curves are exponential decay functions characterizing the loss of ^{13}CO and PO adsorption sites as functions of lysine exposure to the Cu(100) surface.

the Cu(100) surface modified by lysine adsorption at 300 K. These data are taken from the areas under the ^{13}CO TPD spectra in Figure 3b. The dashed line is a fit of the data to a first-order exponential decay and yields a time constant of 109 ± 2 s. Figure 9 also shows the yields of *R*-PO (○) and *S*-PO (◇) adsorbed to the Cu(100) surface as a function of L-lysine exposure. These data are taken from the TPD spectra in Figure 5 using only the area under the high temperature features corresponding to PO interacting with the Cu(100) surface. The curve fit is also a first-order exponential decay and yields a time constant of 65 ± 3 s. The fact that the disappearance of PO adsorption sites occurs roughly twice as rapidly as the loss of CO adsorption sites is simply a reflection of the fact that PO is larger and occupies greater area (more empty sites) in its adsorbed state than CO.

The absolute coverage of CO on the clean Cu(100) surface and the decay of CO adsorption sites with increasing exposure of the Cu(100) surface to lysine can be used to estimate the fraction of empty sites left as a function of lysine exposure. The fact that the coverages of both CO and PO have the same functional dependence on lysine exposure suggests that this is a relevant way to quantify the coverage of available PO adsorption sites. Figure 10 uses this titration of empty sites as the basis of plotting the enantiospecific PO peak desorption temperature differences on the D- and L-lysine modified Cu(100) surfaces. At empty site coverages of θ_O < 0.1, the PO desorption signal is too weak to allow accurate measurements of enantiospecific desorption temperatures. At empty site coverages of θ_O > 0.5, the majority of the adsorbed PO is not interacting with the coadsorbed lysine and thus the enantiospecificity is low. The maximum in the enantiospecificity of *R*- and *S*-PO desorption occurs at a lysine exposure of 150 s and corresponds to a coverage of empty sites (as measure by CO titration) of $\theta_O \approx 0.25$.

dx.doi.org/10.1021/la3027557 | *Langmuir* 2012, 28, 15251−15262

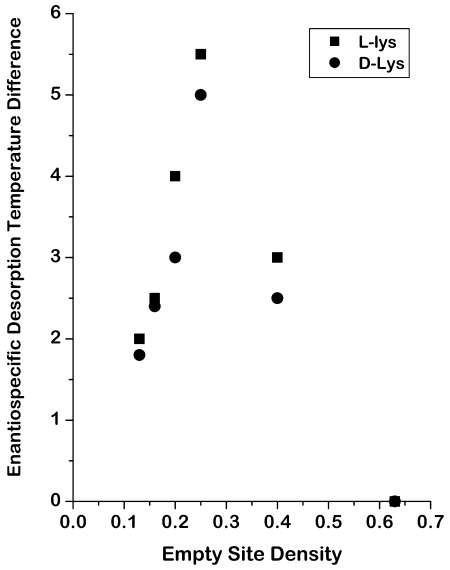

Figure 10. Enantiospecific peak desorption temperature difference (ΔT_p) for *S*- and *R*-PO on L- and D-lysine modified Cu(100) as a function of empty site density after lysine exposure. The peak desorption temperature of *S*-PO was higher than that of *R*-PO for L-lysine modified Cu(100), while the peak desorption temperature of *R*-PO was higher than that of *S*-PO for D-lysine modified Cu(100). The enantiospecific peak temperature difference depends critically on the lysine modifier coverage. ΔT_p reaches a maximum value of 5.5 K at an empty site density of $\theta_O = 0.25$ corresponding to a lysine exposure of 150 s.

The peak PO desorption temperatures measured in this set of experiments are summarized in Figure 11. The data for adsorption on the lysine modified Cu(100) surfaces was obtained using a lysine coverage that yielded $\theta_O \approx 0.25$, the empty site coverage at which we observe the greatest enantiospecific shifts, ΔT_p, in PO desorption temperatures. The values reported in Figure 11 were obtained from the

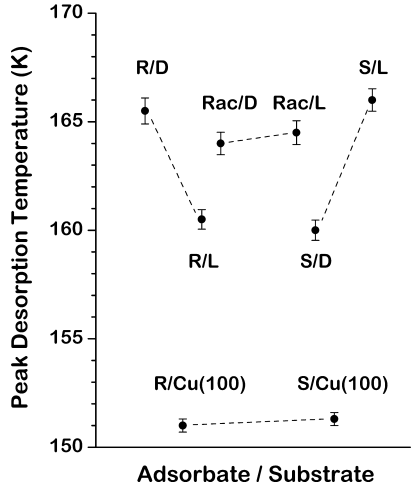

Figure 11. Average peak desorption temperatures of racemic, *S*-, *R*-PO on the L- and D-lysine modified Cu(100) and clean Cu(100) surfaces. Error bars correspond to one standard deviation in the temperature as determined from six repetitions of each TPD experiment. The results on the L- and D-lysine modified Cu(100) reveal a clear and significant diastereomeric effect. The results with racemic PO and on the achiral clean Cu(100) reveal no enantiospecificity.

averages and standard deviations of six independent measurements made for each combination of *R*- or *S*-PO on clean, D- or L-lysine modified Cu(100). In order to determine peak temperatures most accurately, Gaussian curves were fitted to each monolayer desorption peak using data from a temperature range of ±8 K about each peak. The peak desorption temperatures were determined from the maxima of the fitted curves for the peaks. The six repetitions of the measurement of the peak desorption temperature for each of the eight combinations of PO with modified and clean Cu(100) surfaces reveal that the peak desorption temperatures can be determined to an accuracy of $\sigma_{Tp} = 0.5$ K. The accuracy on the clean Cu(100) surface is $\sigma_{Tp} = 0.3$ K. It is clear from the control experiments that there is no significant difference in the peak desorption temperatures of *R*- and *S*-PO from the clean Cu(100) surface and there is no significant difference in the peak desorption temperatures of racemic PO desorbing from the D- or L-lysine modified Cu(100) surface. In contrast, the desorption of *R*- or *S*-PO from D- or L-lysine modified Cu(100) reveals true diastereomerism and thus, enantiospecific adsorption of PO. The enantiospecific shift in the peak desorption temperature is $\Delta T_p = 5.5 \pm 0.5$ K.

The observed enantiospecific difference in PO peak desorption temperatures (ΔT_p) can be used to reveal the corresponding enantiospecific difference in desorption energies, $\Delta\Delta E_{des}$, after estimating the desorption energy (ΔE_{des}) from the peak desorption temperature (T_p). As molecular desorption of PO from the chiral surface can be reasonably approximated using first-order desorption kinetics, the Redhead relation[42] has been used to estimate ΔE_{des} with an assumed pre-exponential factor of $\nu = 10^{13}$ s^{-1}. At maximum enantiospecificity, the values of T_p and ΔE_{des} for each adsorbate/modifier/substrate combination are tabulated in Table 1. While the pre-exponents

Table 1. Enantiospecific Desorption Temperatures and Estimated Desorption Energies for PO on Lysine Modified Cu(100) at the Lysine Coverage Yielding Maximal Enantiospecificity

adsorbate/modifier/Cu(100)	av T_p (K)	avΔE_{des} (kJ/mol)
R-PO/D-lys/Cu(100)	165.5 ± 0.6	43.47 ± 0.16
S-PO/L-lys/Cu(100)	166.0 ± 0.5	43.60 ± 0.14
R-PO/L-lys/Cu(100)	160.5 ± 0.4	42.11 ± 0.12
S-PO/D-lys/Cu(100)	160.0 ± 0.5	41.98 ± 0.12

could be enantiospecific, no attempts were made to evaluate the pre-exponents or to determine their enantiospecificity. Even if some error is associated with the assumed pre-exponential factor, the relative differences in desorption energies between different enantiomer/modifier/substrate combinations are significant. For *S*- and *R*-PO on the L-lysine/Cu(100) and D-lysine/Cu(100) surfaces, $\Delta\Delta E_{des}$ is approximately 2 kJ mol^{-1} at the modifier coverage inducing maximum enantiospecificity. This result is especially encouraging considering our previous failure to observe enantiospecific adsorption of either PO or *R*-3-methylcyclohexanone on Cu(100) and Cu(111) surfaces modified with a variety of chiral species including 2-butanol, 2-butanoxy, alanine, and alaninol.[16] The lysine modified Cu(100) surface is, thus far, the only chirally modified Cu surface to exhibit experimentally detectable enantiospecificity for the desorption of a chiral probe molecule. This enantiospecific difference is the fundamental basis for enantioselective discrimination of chiral compounds.

dx.doi.org/10.1021/la3027557 | *Langmuir* 2012, 28, 15251−15262

4.3. Origin of Enantiospecific Adsorption of PO on Lysine Modified Cu(100). The enantiospecific behavior on the lysine modified surface can occur through several possible chiral induction mechanisms. Because adsorption of PO on achiral Cu surfaces modified by many other modifiers including L-alanine, L-alaninol, 2-butanol, and 2-butoxide species was not enantiospecific,[16] comparison of these chirally modified Cu surfaces with the lysine modified Cu(100) surface should be useful in understanding the probable origin of the observed enantiospecificity. Clearly the central difference between lysine and the other modifiers used is the presence of an additional hydrogen bonding site provided by the amino group in the lysine side chain, $-(CH_2)_4NH_2$. In the case of the L-alanine/Cu(100) system,[16] hydrogen bonding interactions have been suggested to occur between adjacent L-alaninate species to form 2D islands with an ordered structure that cannot accommodate PO. It is possible that the additional amino group in the side chain of lysine offers an extra hydrogen bonding site for the enantiospecific interactions with the epoxide group in PO. In order for this to happen, the amino group has to be adjacent to the epoxide. As the epoxide in PO is involved in the bonding to Cu, the side-chain amino group in lysine is expected to be close enough to the surface. This is consistent with our speculation that lysine adsorbs with its side chain lying flat on the surface when enantiospecificity occurs. Nevertheless, we can not rule out the possibility that this critical hydrogen donor originates from the amino group attached to the chiral carbon. In fact, previous studies of lysine on Cu(110) suggest that lysine adsorbs in its zwitterionic form as a result of proton transfer from the carboxyl group to the α-amino group[34,43] while alanine adsorbs on Cu surfaces as an anion.[11,44] A recent study of the chemical state of lysine on Cu(110) using X-ray photoelectron spectroscopy (XPS) and near-edge X-ray absorption fine structure (NEXAFS) spectroscopy revealed that lysine formed a zwitterion when adsorbed at low temperature but deprotonated after annealing to 420 K.[33] If this is the case, within our investigated low-temperature range, the protonated α-amino group could indeed provide the critical hydrogen bonding site for enantiospecific interactions. This rationale, however, has yet to explain why enantiospecific desorption of PO was highly sensitive to the lysine modifier coverage.

Another interesting finding about the lysine/Cu(100) system not found on many other chirally modified Cu surfaces was the restructuring of the underlying Cu surface to form homochiral (3,1,17) facets through step bunching and faceting.[7] These facets are known to appear at high lysine coverage after annealing at 430 K for 20 min when the lysine molecules are most likely deprotonated. The question now is whether some of these homochiral facets could already be formed at room temperature within the range of lysine coverages where enantiospecificity was observed. While adsorption of glycine, L-alanine, and L-phenylalanine on Cu(100) had caused step faceting and bunching into (3,1,17) facets even at room temperature,[9] these molecules were in the deprotonated forms whereas lysine was believed to be in its zwitterionic form at room temperature. Based on our TPD results, PO desorbs directly from Cu when enantiospecificity occurs. Subsequently arriving PO may not interact directly with underlying Cu on the restructured facets if the facets are covered by a (4×1) lysine overlayer structure.[7] Nevertheless, at intermediate or lower coverages the (3,1,17) facets may have a reduced local coverage of lysine with sufficient void space to accommodate PO. This could explain the enantiospecific desorption of PO directly from Cu. Unfortunately, TPD and LEED experiments cannot provide information about the existence of homochiral (3,1,17) facets on the surface and hence this rationale remains speculative. Future experimental effort can therefore be invested in understanding the coadsorption of lysine and PO on these (3,1,17) facets by investigating the desorption of PO from the naturally chiral Cu(3,1,17) surface similarly modified by single enantiomers of lysine.

5. CONCLUSIONS

Using *R*- and *S*-PO as the probe molecule, enantiospecific adsorption was probed on the D- and L-lysine modified Cu(100) surface. This probe/modifier/metal system was found to exhibit a diastereomeric effect and hence true enantiospecific behavior over a narrow range of lysine coverages. *S*-PO adsorbs more strongly onto the L-lysine/Cu(100) surface than *R*-PO, while *R*-PO adsorbs more strongly onto the D-lysine/Cu(100) surface than *S*-PO. This observed enantiospecificity, however, was found to be critically dependent on the lysine modifier coverage. The enantiospecific temperature difference between *S*- and *R*-PO from the lysine/Cu(100) surface increases with lysine coverage before reaching a maximum of $\Delta T_p \approx 5.5$ K at an empty site coverage of $\theta_O \approx 0.25$. The enantiospecificity then decreases with increasing lysine coverage. Available sites on the surface that can be occupied by PO also diminish at higher lysine coverage. The lysine modified Cu(100) surface is, thus far, the only chirally modified Cu surface which exhibits experimentally detectable enantiospecific effects.

■ ASSOCIATED CONTENT

Ⓢ Supporting Information

Additional figure showing TPD of ^{13}CO on the clean Cu(3,1,17)^S surface at various exposures. This material is available free of charge via the Internet at http://pubs.acs.org.

■ AUTHOR INFORMATION

Corresponding Author

*Telephone: 412-268-3848. E-mail: gellman@cmu.edu.

Notes

The authors declare no competing financial interest.

■ ACKNOWLEDGMENTS

This work has been supported by Department of Energy under Grant No. DE-FG02-12ER16330.

■ REFERENCES

(1) McFadden, C. F.; Cremer, P. S.; Gellman, A. J. Adsorption of chiral alcohols on "chiral" metal surfaces. *Langmuir* **1996**, *12*, 2483−2487.

(2) Cheong, W. Y.; Gellman, A. J. Energetics of Chiral Imprinting of Cu(100) by Lysine. *J. Phys. Chem. C* **2011**, *115*, 1031−1035.

(3) Sholl, D. S.; Asthagiri, A.; Power, T. D. Naturally Chiral Metal Surfaces as Enantiospecific Adsorbents. *J. Phys. Chem. B* **2001**, *105* (21), 4771−4782.

(4) Raval, R. Assembling molecular guidance systems for heterogeneous enantioselective catalysts. *CATTECH* **2001**, *5* (1), 12−28.

(5) Baddeley, C. J. Fundamental investigations of enantioselective heterogeneous catalysis. *Top. Catal.* **2003**, *25*, 17−28.

(6) Chen, Q.; Richardson, N. V. Surface facetting induced by adsorbates. *Prog. Surf. Sci.* **2003**, *73*, 59−77.

(7) Zhao, X.; Zhao, R. G.; Yang, W. S. Scanning tunneling microscopy investigation of L-lysine adsorbed on Cu(001). *Langmuir* **2000**, *16*, 9812−9818.
(8) Zhao, X. Fabricating homochiral facets on Cu(001) with L-lysine. *J. Am. Chem. Soc.* **2000**, *122*, 12584−12585.
(9) Zhao, X.; Wang., H; Zhao, R. G.; Yang, W. S. Self-assembly of amino acids on the Cu(001) surface. *Mater. Sci. Eng., C* **2001**, *16*, 41−50.
(10) Barlow, S. M.; Raval, R. Complex organic molecules at metal surfaces: bonding, organization and chirality. *Surf. Sci. Rep.* **2003**, *50*, 201−341.
(11) Barlow, S. M.; Louafi., S.; Le Roux, D.; Williams, J.; Muryn, C.; Haq, S.; Raval, R. Polymorphism in supramolecular chiral structures of *R*- and *S*-alanine on Cu(110). *Surf. Sci.* **2005**, *590*, 243−263.
(12) Chen, Q.; Frankel, D. J.; Richardson, N. V. Organic adsorbate induced surface reconstruction: *p*-aminobenzoic acid on Cu{110}. *Langmuir* **2001**, *17*, 8276−8280.
(13) Lee, I.; Zaera, F. Chiral templating of surfaces: Adsorption of (*S*)-2-methylbutanoic acid on Pt(111) single-crystal surfaces. *J. Am. Chem. Soc.* **2006**, *128*, 8890−8898.
(14) Raval, R. Creating chiral architectures at metal surfaces. *J. Phys.: Condens. Matter* **2002**, *14*, 4119−4132.
(15) Raval, R. Chiral expression at metal surfaces. *Curr. Opin. Solid State Mater. Sci.* **2003**, *7*, 67−74.
(16) Cheong, W. Y.; Huang, Y.; Dangaria, N.; Gellman, A. J. Probing enantioselectivity on chirally modified Cu(110), Cu(100) and Cu(111) surfaces using temperature programmed desorption. *Langmuir* **2010**, *26* (21), 16412−16423.
(17) Stacchiola, D.; Burkholder, L.; Zheng, T.; Weinert, M.; Tysoe, W. T. Requirements for the formation of a chiral template. *J. Phys. Chem. B* **2005**, *109*, 851−856.
(18) Gao, F.; Wang, Y.; Burkholder, L.; Tysoe, W. T. Enantioselective Chemisorption of Propylene Oxide on a 2-Butanol Modified Pd(111) Surface: The Role of Hydrogen-Bonding Interactions. *J. Am. Chem. Soc.* **2007**, *129*, 15240−15249.
(19) Stacchiola, D.; Burkholder, L.; Tysoe, W. T. Enantioselective chemisorption on a chirally modified surface in ultrahigh vacuum: adsorption of propylene oxide on 2-butoxide-covered palladium(111). *J. Am. Chem. Soc.* **2002**, *124*, 8984−8989.
(20) Stacchiola, D.; Burkholder, L.; Tysoe, W. T. Probing enantioselective chemisorption in ultrahigh vacuum. *J. Mol. Catal. A: Chem.* **2004**, *216*, 215−221.
(21) Ahmadi, A.; Attard, G.; Feliu, J.; Rhodes, A. Surface reactivity at "chiral" platinum surfaces. *Langmuir* **1999**, *15*, 2420−2424.
(22) Horvath, J. D.; Gellman, A. J. Enantiospecific desorption of *R*- and *S*-propylene oxide from a chiral Cu(643) surface. *J. Am. Chem. Soc.* **2001**, *123*, 7953−7954.
(23) Horvath, J. D.; Gellman, A. J. Enantiospecific desorption of chiral compounds from chiral Cu(643) and achiral Cu(111) surfaces. *J. Am. Chem. Soc.* **2002**, *124*, 2384−2392.
(24) Horvath, J. D.; Koritnik, A.; Kamakoti, P.; Sholl, D.; Gellman, A. J. Enantioselective separation on a naturally chiral surface. *J. Am. Chem. Soc.* **2004**, *126*, 14988−14994.
(25) Schillinger, R.; Sljivancanin, Z.; Hammer, B.; Greber, T. Probing enantioselectivity with x-ray photoelectron spectroscopy and density functional theory. *Phys. Rev. Lett.* **2007**, *98*, 136102(1)−136102(4).
(26) Gladys, M. J.; Stevens, A. V.; Scott, N. R.; Jones, G.; Batchelor, D.; Held, G. Enantiospecific adsorption of alanine on the chiral Cu{531} surface. *J. Phys. Chem. C* **2007**, *111* (23), 8331−8336.
(27) Barlow, S. M.; Louafi, S.; Le Roux, D.; Williams, J.; Muryn, C.; Haq, S.; Raval, R. Supramolecular assembly of strongly chemisorbed size- and shape-defined chiral clusters: S- and R-alanine on Cu(110). *Langmuir* **2004**, *20*, 7171−7176.
(28) Chen, Q.; Frankel, D. J.; Richardson, N. V. Chemisorption induced chirality: glycine on Cu{110}. *Surf. Sci.* **2002**, *497*, 37−46.
(29) Gao, F.; Li, Z.; Wang, Y.; Burkholder, L.; Tysoe, W. T. Chemistry of Glycine on Pd(111): Temperature-Programmed Desorption and X-ray Photoelectron Spectroscopic Study. *J. Phys. Chem. C* **2007**, *111*, 9981−9991.
(30) Gao, F.; Li, Z.; Wang, Y.; Burkholder, L.; Tysoe, W. T. Chemistry of Alanine on Pd(111): Temperature-programmed desorption and X-ray photoelectron spectroscopic study. *Surf. Sci.* **2007**, *601*, 3276−3288.
(31) Gao, F.; Wang, Y.; Burkholder, L.; Tysoe, W. T. Chemistry of L-proline on Pd(111): Temperature-programmed desorption and X-ray photoelectron spectroscopic study. *Surf. Sci.* **2007**, *601*, 3579−3588.
(32) Lofgren, P.; Krozer, A.; Lausmaa, J.; Kasemo, B. Glycine on Pt (111): a TDS and XPS study. *Surf. Sci.* **1997**, *370*, 277−292.
(33) Eralp, T.; Shavorskiy, A.; Held, G. The Adsorption Geometry and Chemical State of Lysine on Cu{110}. *Surf. Sci.* **2011**, *605*, 468−472.
(34) Humblot, V.; Methivier, C.; Pradier, C. M. Adsorption of L-lysine on Cu(110): A RAIRS study from UHV to the liquid phase. *Langmuir* **2006**, *22*, 3089−3096.
(35) Andersson, S.; Pendry, J. B. Structure of CO adsorbed on Cu(100) and Ni(100). *Phys. Rev. Lett.* **1979**, *43*, 363−366.
(36) Heskett, D.; Strathy, I.; Plummer, E. W.; de Paola, R. A. Photoemission and electron energy loss spectroscopy investigation of CO+K/Cu(100). *Phys. Rev. B* **1985**, *32*, 6222−6237.
(37) McConville, C. F.; Woodruff, D. P.; Prince, K. C.; Paolucci, G.; Chab, V.; Surman, M.; Bradshaw, A. M. An x-ray absorption and photoelectron diffraction study of the Cu(100) c(2x2) CO structure. *Surf. Sci.* **1986**, *166*, 221−233.
(38) Tracy, J. C. Structural Influences on adsorption energy. 3. CO on Cu(100). *J. Phys. Chem.* **1972**, *56*, 2748.
(39) Vollmer, S.; Wittle, G.; Woll, C. Determination of site specific adsorption energies of CO on copper. *Catal. Lett.* **2001**, *77* (1−3), 97−101.
(40) Wichtendahl, R.; Rodriguez-Rodrigo, M.; Hartel, U.; Kuhlenbeck, H.; Freund, H. J. Thermodesorption of CO and NO from Vacuum-Cleaved NiO(100) and MgO(100). *Phys. Status Solidi A* **1999**, *173*, 93−100.
(41) Jakob, P.; Menzel, D. Initial stages of multilayer growth and structural phase transitions of physisorbed benzene on Ru(001). *J. Chem. Phys.* **1996**, *105* (9), 3838−3848.
(42) Redhead, P. A. Thermal desorption of gases. *Vacuum* **1962**, *12*, 203−211.
(43) Tielens, F.; Humblot, V.; Pradier, C. M. Elucidation of the low coverage chiral adsorption assembly of L-lysine on Cu(110) surface: A theoretical study. *Surf. Sci.* **2008**, *602* (5), 1032−1039.
(44) Jones, G.; Jones, L. B.; Thibault-Starzyk, F.; Seddon, E. A.; Raval, R.; Jenkins, S. J.; Held, G. The local adsorption geometry and electronic structure of alanine on Cu{110}. *Surf. Sci.* **2006**, *600*, 1924−1935.